Quantum Chemical Calculations of Reduction Potentials of AnO_2^{2+}/AnO_2^+ (An = U, Np, Pu, Am) and Fe^{3+}/Fe^{2+} Couples

Satoru Tsushima,[†] Ulf Wahlgren,*,[†] and Ingmar Grenthe[‡]

Institute of Physics, AlbaNova University Center, Stockholm University, 106 91, Stockholm, Sweden, and Department of Chemistry, Royal Institute of Technology (KTH), 100 44 Stockholm, Sweden

The reduction potentials of the $AnO_2(H_2O)_5^{2+}/AnO_2(H_2O)_5^+$ couple (An = U, Np, Pu, and Am) and Fe-$(H_2O)_6^{3+}$ to $Fe(H_2O)_6^{2+}$ in aqueous solution were calculated at MP2, CASPT2, and CCSD(T) levels of theory. Spin—orbit effects for all species were estimated at the CASSCF level. Solvation of the hydrated metal cations was modeled both by polarizable conductor model (PCM) calculation and by solvating the solutes with over one thousand TIP3P water molecules in the QM/MM framework. The redox reaction energy calculated by QM/MM method agreed well with the PCM method after corrections using the classical Born formula for the contribution from the rest of the solvation sphere and correction for dynamic response of solvent polarization in the MM region. Calculated reduction potentials inclusive of spin—orbit effect, zero-point energy, thermal corrections, entropy effect, and PCM solvation energy were found to be comparable with experimental data. The difference between CASPT2 calculated and experimental reduction energies were less than 35 kJ/mol in all cases, which ensures that CASPT2 (and CCSD(T)) calculations provide reasonable estimates of the thermochemistry of these reactions.
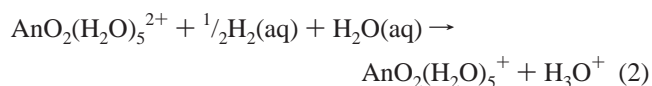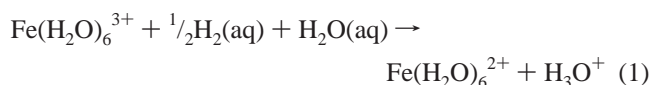
1. Introduction

The chemical properties of actinides are very similar when they are in the same oxidation state; however, there are significant differences in their redox properties.[1] This fact is very important in technology and is used in the design of chemical separation processes in the reprocessing of spent nuclear fuel and for understanding the speciation and migration behavior of actinides in surface and groundwater systems. Complex formation reactions involving actinides are, in general, very fast, whereas redox reactions can be slow, particularly when there is a large change in structure between the reduced and oxidized form, as between An^{4+} and AnO_2^+ or AnO_2^{2+}. The experimental study of the chemistry of the actinides is far from simple and requires special laboratory facilities; it is therefore important to explore if and how theoretical methods can be used as an "experimental" tool—this is the purpose of the present article and the related communication.[2]

The equilibrium and kinetics of the U(VI)—Fe(II) to U(V)—Fe(III) redox process was studied experimentally by Tomiyasu et al.,[3] reviewed by Newton,[4] and studied theoretically by Privalov et al.[5] Reduction of UO_2^{2+} by Fe^{2+}; i.e., the reaction $UO_2^{2+}(aq) + Fe^{2+}(aq) \rightarrow UO_2^+(aq) + Fe^{3+}(aq)$ is an endergonic process with standard Gibbs energy change of the reaction $\Delta G°$, +65.9 kJ/mol. [Estimated for zero ionic strength using reduction potentials for UO_2^{2+}/UO_2^+ of 0.088 V (ref 6) and for Fe^{3+}/Fe^{2+} of 0.771 V (refs 7 and 8).] However, UO_2^{2+} and Fe^{3+} (especially the latter) hydrolyze in water, forming species such as $UO_2(OH)_n^{2-n}$ and $Fe(OH)_n^{3-n}$; this results in a change in the redox potential of the system and facilitates the reduction of U(VI) by Fe(II).

In a number of previous papers[9–14] we have explored how the calculated results depend on the quantum chemical ap-

proximations used. In the present article we have studied the redox reactions involving the couples $AnO_2(H_2O)_5^{2+}/AnO_2$-$(H_2O)_5^+$ (An = U, Np, Pu, and Am) and $Fe(H_2O)_6^{3+}/Fe(H_2O)_6^{2+}$ in aqueous solution.

The reduction potentials are obtained from the calculated Gibbs energy changes of the reactions

$$Fe(H_2O)_6^{3+} + {}^1/_2H_2(aq) + H_2O(aq) \rightarrow$$
$$Fe(H_2O)_6^{2+} + H_3O^+ \quad (1)$$

$$AnO_2(H_2O)_5^{2+} + {}^1/_2H_2(aq) + H_2O(aq) \rightarrow$$
$$AnO_2(H_2O)_5^+ + H_3O^+ \quad (2)$$

There are several problems in calculating the reduction potentials. First and foremost this concerns the solvent effects. In the left-hand side of reaction 1 there is one reactant with charge +3 whereas in the right-hand side there is one double charged ion and a H_3O^+ ion. Similarly, reaction 2 involves one double charged reactant and a single charged ion and H_3O^+ as products. The solvent effect on the reaction can thus be expected to be large, and accurate estimates of the solvation energies, or rather of the solvation energy differences, are crucial. The inclusion of a first hydration shell is of course mandatory, but even so the solvent effect on the reaction energy is very large (of the order of 700 kJ/mol for reaction 1), much larger than the reaction energy itself. Solvent effects can be described by including a large number of water molecules in the calculation for the highly charged ions. Alternatives are provided by models where the solvent is described by a polarizable continuum model (PCM), hybrid models such as QM/MM, or molecular dynamics (MD) models. In the present study we have calculated the solvent effect using a PCM model on complexes with a saturated first hydration shell. To establish the accuracy of this model we also calculated the reaction energy for the iron—uranyl

* Corresponding author. E-mail: uw@physto.se.
† Stockholm University.
‡ Royal Institute of Technology.

system (eq 3) by the QM/MM model, and including corrections for the long range solvent effect and the polarization of the water molecules using the Born formula.

$$UO_2(H_2O)_5^{2+} + Fe(H_2O)_6^{2+} \rightarrow UO_2(H_2O)_5^+ + Fe(H_2O)_6^{3+}$$
(3)
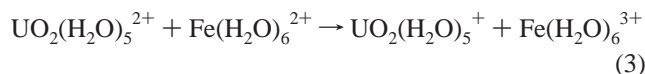
Because the number of unpaired electrons on the metal complexes changes during the reactions, it is important to include spin−orbit effects; this is feasible for complexes of the type studied here.

Shamov et al.[15] have recently studied $AnO_2(H_2O)_5^{2+}/AnO_2(H_2O)_5^+$ (An = U, Np, Pu) reduction potentials using B3LYP hybrid density functional theory with small core effective core potentials (ECPs) on actinides and PCM on the solvent, and obtained Gibbs energies which are in satisfactory agreement with experiment. In a previous study by the same authors, where they used large core ECPs,[16] less satisfactory results were reported; this suggests that it is important to use small core ECPs to calculate reliable thermochemical data. The reduction potential of $Fe(H_2O)_6^{3+}$ to $Fe(H_2O)_6^{2+}$ has been studied by Li et al.[17] and Uudsemaa et al.[18] using DFT/PCM calculations. These authors were not able to get satisfactory results when only first hydration shell was included in solute model. However, this is not in agreement with the present findings.

It is well-known that SCF underestimates the internal "-yl" bond distances in $AnO_2(H_2O)_n^{2+/+}$ complexes. In the present study we have therefore chosen to optimize geometries at the UMP2 level. However, there is an uncertainty associated with energies calculated using an unrestricted one-configuration method on complexes where multireference effects are large, which is the case for the actinide complexes with more than one open f-shell as in the present study. Reduction potentials were instead calculated using the CASPT2 method with only the most important configurations included in the active space (minimal CASPT2). To ascertain the quality of the results, we have also calculated the reduction potentials at the CCSD(T) level for the systems that can be described by one configuration (the iron and uranyl complexes).

2. Details of the Calculations

Calculations were performed using Gaussian 03 [19] and MOLCAS 6.[20] Effective core potentials (ECPs) were used on the actinides and iron. The actinides were described by the small core ECPs, suggested by Küchle et al.,[21] comprising 60 electrons in the core, with corresponding basis sets. For iron, the ECP with 10 electrons in the core suggested by Dolg et al.[22] and the corresponding basis set were used. The actinide basis sets were supplemented with two g-functions and the iron basis set with one f-function. Oxygen was described at the all-electron level with a (12s,6p,1d) primitive set of Gaussians contracted to (5s,4p,1d) basis.[23] For hydrogen, a 5s contracted to 3s basis set was used[23] in the geometry optimizations, whereas a p-function was added to the hydrogen basis in the energy calculations. Geometry optimizations were done in gas phase at the unrestricted MP2 level using Gaussian 03 without symmetry constraints.

In the actinide complexes multireference effects originating from strong couplings in the bare ion occur in all complexes with more than one unpaired f-electron. Reaction energies were calculated at the CASPT2 level because energies calculated with any unrestricted method are unreliable for strongly multiconfigurational systems such as the higher actinides. Only the most important configurations, arising from redistributions of the electrons in the low-lying f-shells, were included in the reference. To assess the accuracy of the minimal-CASPT2 method, calculations at the CCSD(T) level using the same basis sets were carried out for the complexes that can be described by one configuration, i.e., the iron and uranyl complexes. In both the CASPT2 and the CCSD(T) calculations the inner core was kept frozen; that is, no excitations from the An (5s,5p,5d) and Fe (3s,3p) shells were included.

The spin−orbit effects were calculated within the variation-perturbation scheme using the RASSI-SO module in MOLCAS 6 program, with a basis set of eight spin-free states obtained from CASSCF calculations using averaged orbitals. The spin−orbit integrals were calculated in the mean-field approximation[24] with the AMFI program.[25] For the actinides, with the exception of Am, the spin−orbit calculations were done at the ECP level[26] using the integral mapping procedure.[27] To use this mapping, the basis sets must be generally contracted. Such basis sets were not available for Am and Fe, and for these elements the SO calculations were done at the all-electron level. Because the spin−orbit effect is sensitive to degeneracies, the CASSCF calculations were done without symmetry to avoid artificial symmetry breaking due to the use of only Abelian symmetry groups in the MOLCAS program.

Solvation energies were calculated in the PCM approximation with a saturated first hydration shell, and for comparison, with the QM/MM model on $Fe(H_2O)_6^{3+/2+}$ and $UO_2(H_2O)_5^{2+/+}$ complexes. In the first case, the solvation energies, which should not be strongly dependent on the multiconfigurational character of the wave function, were calculated at the UMP2 level with Gaussian 03, using the Conducting Polarizable Continuum model (CPCM).[28]

The aim of QM/MM calculations was to investigate the reliability of the PCM model. The calculations were done using the two-layer ONIOM framework [29] implemented in Gaussian 03, with the metal ion and a saturated first hydration shell defining the QM region and 1304 (11^3-3^3) solvent water molecules for the MM region. For the initial structure, solvent water molecules (MM waters) were periodically located around the solute with the nearby oxygen−oxygen atomic distance equal to 3.00 Å. The full geometry (solute + solvent) was allowed to fully relax during the QM/MM geometry optimization. Because the aim of the calculations was to investigate the reliability of the PCM model rather than to obtain accurate reaction energies, they were calculated at the UMP2 level using a large core ECP on uranium (with 78 electrons in the core).[30] The resulting loss in accuracy was quite small, 15 kJ/mol for the reaction energy of eq 3, whereas the error using UMP2 was somewhat larger, 35 kJ/mol, for the same reaction calculated within the PCM model. However, these errors are inconsequential considering the aim of the calculations.

We used rigid TIP3P waters[31] as solvent molecules for the MM part of the QM/MM calculations. Nonbonding Lennard-Jones parameters for the iron−water interaction were taken from literature.[32] For nonbonding and bonding (U−O_{yl} and O_{yl}−U−O_{yl}) interactions of uranyl (VI) and uranyl (V), we used force field parameters developed by Guilbaud et al.[33] For the central metal cation and solute water molecules, charges taken from Mulliken population analysis were used. ONIOM calculation incorporates the partial charges of MM region into the QM Hamiltonian. This allows the QM wave functions to be polarized and better describes the electrostatic interaction between QM and MM parts.

The use of 1304 water molecules corresponds to about 15 Å around the solute molecules (i.e., 30 Å box size), but this is

clearly too small to describe the long-range Coulomb interaction between the solute and the solvent. We have therefore added the contribution from the solvent outside the MM sphere using the classical Born formula:[34]

$$\Delta G_{solv} = -\frac{q^2}{2r}\left(1 - \frac{1}{\epsilon}\right) \qquad (4)$$

where q is the charge of the solute, r is its ionic radius, and ϵ is the dielectric constant of the medium (the dielectric constant of water at 25 °C is $\epsilon = 78.39$).

The TIP3P potential does not account for the relaxation of the charge distribution of the water molecule in the electrostatic field of the solute ion, and the dynamic response of the solvent is thus is not properly accounted for in this model. This effect, which is quite large, can be estimated as follows. The dynamic dielectric constant in water, ϵ_∞, describes the contribution of the electronic response to the total solvent effect. This contribution from the MM part of the solvent can be estimated from the Born formula by first calculating the total effect in a sphere containing the metal ion and all water molecules including the first hydration sphere, and then subtracting the contribution from the metal and the first hydration sphere:

$$\Delta G_{solv(dynamic)} = -\frac{q^2}{2r_1}\left(1 - \frac{1}{\epsilon_\infty}\right) + \frac{q^2}{2r_2}\left(1 - \frac{1}{\epsilon_\infty}\right) \qquad (5)$$

where r_1 is the radius of the QM solute (e.g., $UO_2(H_2O)_5^{2+}$), r_2 is the radius of the QM+MM solute (e.g., $UO_2(H_2O)_5$-$(H_2O)_{1304}^{2+}$), and ϵ_∞ is the dynamic dielectric constant of water ($\epsilon_\infty = 1.78$).

Zero-point energy corrections and thermal corrections (vibrational, rotational, and translational) and contribution from entropy were calculated using classical formulas for the rotational and translational contributions and a vibrational frequency analysis for the vibrational part. The vibrational frequencies were calculated at the SCF level in the gas phase using large core ECPs on U, Np, and Pu.[30] The partition function is quite robust, and the errors associated with the approximations should be of minor importance. The total electronic contribution to the entropy from the ground state is given by $S_{elec} = R\ln(g)$, where R is the gas constant and g is the spin multiplicity. No electronic contributions to the entropy originating from low-lying excited states were considered. Because $AmO_2(H_2O)_5^{2+/+}$ were found to be unstable in the gas phase at the SCF level, as was previously pointed out by Vallet et al.,[35] we were not able to estimate thermal contributions for the $AmO_2(H_2O)_5^{2+/+}$ couple and these effects are not included in final reaction energy and reduction potential for this system.

3. Results and Discussions

3.1. Structures of $Fe(H_2O)_6^{3+/2+}$ and $AnO_2(H_2O)_5^{2+/+}$. Structures of $Fe(H_2O)_6^{3+/2+}$ and $AnO_2(H_2O)_5^{2+/+}$ (An = U, Np, Pu, and Am) were optimized at the UMP2 level with and without symmetry constraints. The results are summarized in Table 1, where we also have included published EXAFS data.[14,36–41] More details are shown in Supporting Information (Table S1), where we, for reference purposes, have included results obtained with an ECP on oxygen. The calculations show a significant contraction of the $An-O_{yl}$ bond from U to Am, 0.10 Å for $AnO_2(H_2O)_5^{2+}$ and 0.05 Å for $AnO_2(H_2O)_5^+$. The geometries were quite sensitive to polarizing functions in the basis sets; for instance, the $U-O_{yl}$ bond distances in $UO_2(H_2O)_5^{2+}$ obtained with and without polarizing functions

TABLE 1: Comparison of Theoretically Calculated and Experimentally Measured Metal–Oxygen Bond Distances (in Ångstrom) in $[Fe(H_2O)_6]^{3+/2+}$ and $[AnO_2(H_2O)_5]^{2+/+}$ (An = U, Np, Pu, Am)

M	oxidation state	MP2		EXAFS	
		$M-O_{ax}$	$M-O_{eq}$	$M-O_{ax}$	$M-O_{eq}$
Fe	II	2.14		2.10[a]	
	III	2.04		2.02[a]	
U	V	1.81	2.51	NA	NA[h]
	VI	1.76	2.44	1.77[b]	2.41[b]
				1.76[c]	2.41[c]
				1.77[d]	2.42[d]
Np	V	1.77	2.49	1.85[c]	2.50[c]
				1.82[e]	2.49[e]
	VI	1.73	2.42	1.75[e]	2.42[e]
Pu	V	1.74	2.49	1.84[f]	2.45[f]
				1.81[g]	2.47[g]
	VI	1.71	2.41	1.74[f]	2.45[f]
				1.74[g]	2.40[g]
Am	V	1.71	2.51	NA	NA
	VI	1.71	2.43	NA	NA

[a] Benfatto et al.[36]   [b] Vallet et al. [14]   [c] Allen et al.[37]   [d] Thompson et al.[38]   [e] Reich et al.[39]   [f] Ankudinov et al.[40]   [g] Conradson et al.[41]   [h] NA: data not available.

in the basis set were 1.763 and 1.822 Å, respectively. Basis set effects in the actinides are discussed in detail elsewhere.[42] We also found that the results were insensitive to the size of the frozen core in the UMP2 calculations, the bond distances changed by at most 0.001 Å when excitations from the remaining core (5s, 5p and 5d) were included in the UMP2 calculations.

3.2. Reduction Potentials. PCM Model Results. Standard Gibbs energy changes, $\Delta G°$, were calculated for reactions 1 and 2 for An = U, Np, Pu, and Am.

Reaction energies for all reactions were calculated at the minimal CASPT2 level; the vibrational frequencies, needed to obtain the thermal functions, were calculated at the SCF level in the gas phase; and the solvent effects were calculated at the UMP2 level as described in the method section. This information and the calculated Gibbs energy changes are shown in Table 2 together with experimental results. In addition, the reaction energies were calculated at the CCSD(T) level for $Fe(H_2O)_6^{3+/2+}$ and $UO_2(H_2O)_5^{2+/+}$ with symmetry constraints, D_{2h} and D_{5h}, respectively.

The gas-phase reaction energies obtained at the CASPT2 and the CCSD(T) levels are shown in the columns a and b in Table 2. For the iron reaction the reaction energy obtained at the CCSD(T) level is 23 kJ/mol lower than that obtained at the CASPT2 level, whereas for the uranyl reaction, CCSD(T) gave a reaction energy that was 8 kJ/mol higher. This result, which is in line with the results quoted in ref 42, indicate an error of the order of 20 kJ/mol associated with the minimal CASPT2 method.

The ground state of Fe^{3+} is ^6S and the ground state of Fe^{2+} is ^5D. There is no first-order spin–orbit effect in the ^6S state, and the total spin–orbit effect in $Fe(H_2O)_6^{3+}$ is, as expected, quite small, 0.2 kJ/mol. A larger spin–orbit effect is expected for Fe^{2+} in the ^5D state, which is split into five multiples in first order. The calculated energy lowering in the bare Fe^{2+} ion due to the spin–orbit interaction is 5.4 kJ/mol whereas the experimental result, assuming the Landé interval rule to hold, is 5.1 kJ/mol. The calculated spin–orbit splitting in the hydrated ion is only 1.6 kJ/mol, which means that the quenching by the coordinated waters is significant. The spin–orbit effect on the reaction energy in the $Fe(H_2O)_6^{3+/2+}$ pair is consequently small (column c Table 2).

TABLE 2: Calculated and Experimental Fe(III)/Fe(II) and An(VI)/An(V) Reduction Energies and the Separate Contributions from Spin−Orbit, Temperature Corrections and Solvation (unit in kJ/mol)[a]

reaction	(a) ΔE CASPT2	(b) ΔE CCSD(T)	(c) $\Delta(\Delta E)$ spin−orbit	(d) $\Delta G(\Delta H)$ correction	(e) $\Delta(\Delta G)$ solvation	(f) $\Delta G^\circ_{(aq)}$ ($\Delta H^\circ_{(aq)}$)		
						CASPT2 (a + c + d + e)	CCSD(T) (b + c + d + e)	exp
$Fe(H_2O)_6^{3+} + 0.5H_2 + H_2O \rightarrow$ $Fe(H_2O)_6^{2+} + H_3O^+$	−764.8	−741.8	−1.4	+5.2 (+12.2)	+693.8	−67.2 (−60.2)	−44.2 (−37.2)	−74.4 (−42.7)
$UO_2(H_2O)_5^{2+} + 0.5H_2 + H_2O \rightarrow$ $UO_2(H_2O)_5^+ + H_3O^+$	−78.2	−86.5	−28.3	+10.0 (+14.2)	+96.8	+0.3 (+4.5)	−8.0 (−3.8)	−8.5 (−6.1)
$NpO_2(H_2O)_5^{2+} + 0.5H_2 + H_2O \rightarrow$ $NpO_2(H_2O)_5^+ + H_3O^+$	−223.9		−39.6	+14.0 (+20.9)	+102.4	−147.1 (−140.2)		−111.8 (−117.4)
$PuO_2(H_2O)_5^{2+} + 0.5H_2 + H_2O \rightarrow$ $PuO_2(H_2O)_5^+ + H_3O^+$	−215.8		+27.7	+4.6 (+11.1)	+113.1	−70.4 (−63.9)		−90.3 (−88.1)
$AmO_2(H_2O)_5^{2+} + 0.5H_2 + H_2O \rightarrow$ $AmO_2(H_2O)_5^+ + H_3O^+$	−310.7		+17.9		+110.0	−182.8[b]		−153.5

[a] Experimental values refer to refs 6−8. [b] No thermal correction added.

TABLE 3: Ground State Configurations of $[AnO_2(H_2O)_5]^{2+/+}$ (An = U, Np, Pu, Am) Obtained by Single-Configurational Calculations without Spin−Orbit Effect, and Those Obtained by Multiconfigurational Calculations with Spin−Orbit Coupling[a]

		single configurational without SO	multiconfigurational with SO	ΔE_{SO}
$[UO_2(H_2O)_5]^{2+}$	f^0			
$[UO_2(H_2O)_5]^+$	f^1	δ^1	δ^1	−28.3
$[NpO_2(H_2O)_5]^{2+}$	f^1	δ^1	δ^1	−31.2
$[NpO_2(H_2O)_5]^+$	f^2	δ^2	$\delta^1\phi^1$	−70.8
$[PuO_2(H_2O)_5]^{2+}$	f^2	δ^2	$\delta^1\phi^1$	−78.8
$[PuO_2(H_2O)_5]^+$	f^3	$\delta^2\phi^1$	$\delta^1\phi^1\pi^1$	−51.1
$[AmO_2(H_2O)_5]^{2+}$	f^3	$\delta^2\phi^1$	$\delta^1\phi^1\pi^1$	−82.8
$[AmO_2(H_2O)_5]^+$	f^4	$\delta^2\phi^2$	$\delta^2\phi^1\pi^1$	−64.9

[a] Spin−orbit (SO) effect relative to the spin-free CASSCF ground state is also shown (unit in kJ/mol).

For the actinides, the spin−orbit correction is significant, and one would expect it to increase with an increasing number of unpaired f-electrons. This holds for uranium (where the energy lowering of the ground state due to spin−orbit interactions for the hexavalent complex is zero) and for neptunium. For Pu and Am the spin−orbit effect is larger in the hexavalent complexes, as shown by the increase in the reaction energy (Table 2 (c)). The reason for this behavior is not clear to us, but it is probably different for Pu and Am. The f-electron configuration for PuO_2-$(H_2O)_5^{2+}$ is $\delta^1\phi^1$ (Table 3) and the additional electron in PuO_2-$(H_2O)_5^+$ enters an f_π orbital, giving rise to a $\delta^1\phi^1\pi^1$ electron configuration. This result agrees with results obtained by Hay et al.[16] from a single-configurational DFT calculation, where they found a $\delta^2\phi^1$ ground state which changed to $\delta^1\phi^1\pi^1$ in a spin−orbit CI calculation. Matsika et al.[43] claim that they have found $\delta^2\phi^1$ as the ground state of PuO_2^+, but details of the calculation are not given in their paper.

The f_π orbital will mix with the p-orbitals on oxygen, and thus to some extent occupy another region of the molecule. One would expect the spin−orbit interaction to decrease in all configurations with an occupied f_π orbital; in addition, the splitting between states with an occupied and an empty f_π orbital will be large. It is conceivable that this may cause the total spin−orbit effect to decrease in Pu(V).

Concerning the Am complexes, the electronic configuration of $AmO_2(H_2O)_5^{2+}$ is $\delta^1\phi^1\pi^1$ whereas it is $\delta^2\phi^1\pi^1$ for AmO_2-$(H_2O)_5^+$. In the LS coupling scheme, a δ^2 configuration gives rise to the states $^3\Sigma^-$, $^1\Sigma^+$ and $^1\Gamma$, none of which is subject to a first-order spin−orbit coupling, and the presence of these states may be the reason for the smaller effect in Am(V) compared to Am(VI).

The enthalpy and Gibbs energy corrections to the electronic energy are shown in column d in Table 2. The thermal corrections are not large; in fact, they are smaller than the uncertainty caused by the CASPT2 approximation. The enthalpy contribution (the number in parentheses in column d, Table 2) is somewhat larger than the Gibbs energy contribution. The calculated entropy, constant volume molar heat capacity, thermal correction to the enthalpy and Gibbs energy of all complexes are given in Table S2 in Supporting Information. The calculated ion entropies of $AnO_2(H_2O)_5^{2+/+}$ in the gas phase are quite different from experimental values for $AnO_2^{2+/+}$(aq). However, the entropy *difference* between An(VI) and An(V) in the gas phase is in reasonable accord with the experimental values, e.g., calculated 65 J/(mol·K) vs experimental 73 J/(mol·K) for the U(VI)/U(V) couple (Table S2). This is important, because it is much more complicated to calculate the thermal functions in the solvent than in the gas phase. It was found in the present study that translational and rotational contributions to the entropy of the reaction for the An(VI)/An(V) reduction is about 1 J/(mol·K) in the gas phase (Table S3 in Supporting Information), which suggests that the contribution is also small in the solvent. It may also be noted that the entropy term *ST* has a significant effect on the thermodynamics of the An(VI) to An(V) reactions, which is caused mostly by vibrational contribution to the entropy and small part from electronic contribution to the entropy.

The solvent contribution is by far the most important correction to the gas-phase reaction energies. The solvation energies of all solutes were calculated separately at the UMP2 level using the gas-phase optimized geometries, using UAHF radii (united atom topological model applied on radii optimized for the HF level) for the atoms in the solute. The solvent effect, shown in column e, Table 2, is very large, about 700 kJ/mol for the iron reaction and about 100 kJ/mol for the actinide reactions. The reason for the very large effect on iron is that the Fe^{3+} ion has a much larger polarization effect than the other ion, due to its small ionic radius and high charge. The effect is smaller for the actinyl ions, which have a lower charge. The solvation energy is ion size dependent and a slight change in ionic radius, which is a parameter during the calculation, can change the solvation energy substantially; this is particularly serious for the iron reaction. However, because we are discussing the relative energy difference between $Fe(H_2O)_6^{3+}$ and Fe-$(H_2O)_6^{2+}$, we can expect a partial cancellation of errors in the solvation energy and the reaction energy will thus be more precise than the absolute energies of reactants and products.

When calculating solvent effects with the PCM model, one must consider that the theoretical solvation energy will depend on the level of theory used in the calculation. In Table 4 we show the solvation energy difference between $AnO_2(H_2O)_5^{2+}$ and $AnO_2(H_2O)_5^+$ at SCF, MP2, and B3LYP levels. The calculated solvation energy contribution to the reduction reac-

Reduction Potentials of AnO₂²⁺/AnO₂⁺

J. Phys. Chem. A, Vol. 110, No. 29, 2006 **9179**

TABLE 4: Solvation Energy Difference between $AnO_2(H_2O)_5^{2+}$ and $AnO_2(H_2O)_5^+$ at Different Levels of Theory (B3LYP value from Ref 15, in kJ/mol)

	MP2	SCF (MP2 geometry)	B3LYP	B3LYP (Prioda[a] geometry)
U	515.8	503.8	519	512
Np	521.5	510.8	531	524
Pu	533.5	523.7	528	534
Am	517.7	520.7		

[a] Four-component all-electron relativistic calculations (ref 15).

TABLE 5: Calculated Fe(III)/Fe(II) and An(VI)/An(V) Gas Phase Reduction Energies at UMP2 and CASPT2 Levels (in kJ/mol)

	ΔE MP2	ΔE CASPT2
$Fe(H_2O)_6^{3+} + 0.5H_2 + H_2O \rightarrow$ $Fe(H_2O)_6^{2+} + H_3O^+$	−800.0	−764.8
$UO_2(H_2O)_5^{2+} + 0.5H_2 + H_2O \rightarrow$ $UO_2(H_2O)_5^+ + H_3O^+$	−64.4	−78.2
$NpO_2(H_2O)_5^{2+} + 0.5H_2 + H_2O \rightarrow$ $NpO_2(H_2O)_5^+ + H_3O^+$	−143.3	−223.9
$PuO_2(H_2O)_5^{2+} + 0.5H_2 + H_2O \rightarrow$ $PuO_2(H_2O)_5^+ + H_3O^+$	−251.9	−215.8
$AmO_2(H_2O)_5^{2+} + 0.5H_2 + H_2O \rightarrow$ $AmO_2(H_2O)_5^+ + H_3O^+$	−318.9	−310.7

tions is smaller at the SCF level than at the correlated levels for all the actinide reactions. Dynamic correlation will in general give rise to more compact charge distributions compared to SCF results, because the electron−electron repulsion is decreased. This effect will be more pronounced the higher the charge on the ion. One would thus expect a higher solvation contribution at the correlated level for the doubly charged ion compared to the singly charged ion, in agreement with the results presented in Table 4. It is noteworthy that the solvation energies obtained at the different correlated levels (MP2 and B3LYP) agree quite well.

The total reaction energy of reactions 1 and 2 at the CASPT2 and CCSD(T) levels are given in columns f of Table 2, together with available experimental data. The agreement between theory and experiment is within 35 kJ/mol. For the iron reaction, the CASPT2 result is in better agreement with experiment than the CCSD(T) result, but this may well be due to some errors in the very large solvent contribution for iron. The results are thus satisfactory, but the large solvent effects are a cause for concern as they increase the uncertainty in the calculated thermodynamic data.

The uncertainty in experimental thermodynamic data for ionic species is, in general, very small, with the exception of ion entropies, the experimental entropy value of $PuO_2^{2+}(aq)$ has an error of 22 J/(mol·K) (Table S2), whereas $\Delta G°$ of the plutonyl-(VI) reduction at 25 °C is much more precise, less than 1 kJ/mol. The calculated enthalpy change ($\Delta H°$) for the reactions U(VI)/U(V) and Fe(III)/Fe(II) at the CCSD(T) level are both within 5 kJ/mol of the experimental value.

In Table 5 reaction energies calculated at the unrestricted MP2 and the CASPT2 levels are compared. It is difficult to estimate the accuracy of unrestricted calculations a priori, because part of the error induced by the single determinant description is corrected by the spin polarization and this effect is difficult to estimate. It is evident from the results in Table 5 that this error is unpredictable. In the iron reaction, where both the Fe²⁺ and the Fe³⁺ complexes should be well described by a single configuration, the difference is 35 kJ/mol. The UMP2 result for the Gibbs energy of reaction is thus 32 kJ/mol, compared to the CASPT2 result, 67 kJ/mol, and the experimental value,

TABLE 6: Calculated Reduction Potentials of $Fe(H_2O)_6^{3+/2+}$ and $AnO_2(H_2O)_5^{2+/+}$ (An = U, Np, Pu, Am) Couples versus Experimental Values (in V)[a]

	CASPT2	CCSD(T)	B3LYP	Prioda[b]	experimental
Fe	0.696	1.119	1.92		0.771
U	0.003	0.082	−0.10	−0.51	0.088
Np	1.525		1.72	0.87	1.159
Pu	0.730		1.29	0.43	0.936
Am	1.894				1.591

[a] B3LYP and Prioda values are from refs 15 and 18 and are corrected for multiplet and spin−orbit effects for U, Np, and Pu pairs. Experimental values refer to refs 6−8. [b] Four-component all-electron relativistic calculations (ref 15).
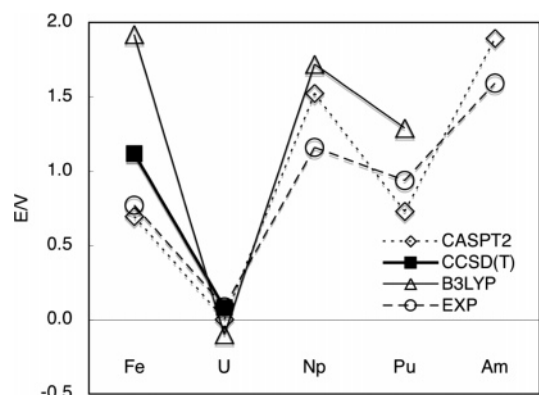
Figure 1. Calculated and experimental reduction potentials of $Fe(H_2O)_6^{3+/2+}$ and $AnO_2(H_2O)_5^{2+/+}$ (An = U, Np, Pu, Am) couples. CASPT2 (diamonds) and CCSD(T) (filled squares) values are from this study. B3LYP (triangles) values are taken from ref 15 and 17. Experimental values (circle) are from refs 6−8.

74 kJ/mol. The agreement is good for uranium, as expected for U(V) that has a single unpaired electron. For neptunium the difference is 81 kJ/mol, making the reaction more endothermic, which is an expected result because Np(VI) has one and Np(V) two unpaired f-electrons and the latter must therefore be described by two configurations. The errors are much smaller for both Pu and Am, presumably because of cancellation of errors. It is evident from the iron results that spin-restricted calculations cannot correct for these errors.
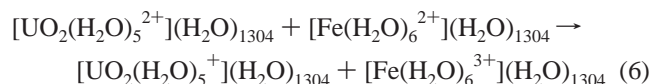
In Table 6 and Figure 1, calculated reduction potentials obtained from (multireference) CASPT2, single-reference B3LYP and four-component all electrons relativistic calculations[15] are compared. It is evident that the single determinant iron system is not well described by B3LYP; the error in the computed redox potential is 1.1 V compared to 0.07 V for the CASPT2 calculation. However, it is somewhat surprising that the CCSD-(T) result is less satisfactory than the CASPT2 result, with an error of 0.35 V compared to experiment. The behavior of the uranyl system is more according to expectations, with errors (compared to experiment) of about 0.1 V. For the Np and Pu reactions, the agreement between the B3LYP results and experiment is reasonable although clearly inferior to the CASPT2 results.

Li et al.[17] and Uudsemaa et al.[18] claim that the inclusion of a second hydration shell is mandatory for getting accurate energies when the redox potential of the M³⁺/M²⁺ transition metals is calculated at the DFT level with the PCM solvation model. Including only the first hydration shell, they found that the B3LYP/PCM method tends to overestimate the reduction potential by about 1−1.5 V. However, contrary to this, Martin et al.[44] obtained accurate thermodynamic data of $Fe(H_2O)_6^{3+}$ ion hydration and hydrolysis reactions using B3LYP calculation

in combination with a numerical solution of a dielectric model. It is not straightforward to compare the result by Martin et al. and our result because we use different solvation models; in addition, iron in their study does not change oxidation states. In the present study, where CASPT2 and CCSD(T) were used to calculate energies, we obtained reasonably good redox potentials with only the first hydration shell, the rest of the solvent being described by the PCM model, which is at variance with statements made by Li et al.[17] and Uudsemaa et al.[18] Their problems are more likely to be associated with unrestricted B3LYP and standard PCM procedures.

3.3. Reduction of U(VI) by Fe(II). To investigate the reliability of the PCM model, we have calculated the reaction energy for the reaction $UO_2^{2+}(aq) + Fe^{2+}(aq) \rightarrow UO_2^+(aq) + Fe^{3+}(aq)$ using both the PCM and the QM/MM models. This reaction is interesting in its own right and is the subject of a separate study,[2] but in the present context it was chosen primarily because the reactant and the product only involves metal complexes and not H_2, H_2O and H_3O^+, which are not central to our solvation problem.

In the QM/MM calculations we used a two-layer ONIOM framework as implemented in Gaussian 03. The solutes were immersed in a water box where a total of 1304 TIP3P waters were positioned around the solute, and the reactions considered can thus be written

$$[UO_2(H_2O)_5{}^{2+}](H_2O)_{1304} + [Fe(H_2O)_6{}^{2+}](H_2O)_{1304} \rightarrow$$
$$[UO_2(H_2O)_5{}^{+}](H_2O)_{1304} + [Fe(H_2O)_6{}^{3+}](H_2O)_{1304} \quad (6)$$

Both the geometry optimizations and the energy calculations were done at the UMP2 level for the solutes ($Fe(H_2O)_6{}^{3+/2+}$ and $UO_2(H_2O)_5{}^{2+/+}$). As discussed in the previous section, UMP2 sometimes does not give accurate results for reaction energies. However, the aim of this investigation is to compare the QM/MM and the PCM models, and the absolute reaction energies are thus less interesting than the relative ones for which the UMP2 method should give satisfactory results. The geometry optimization was performed in a fully static way, which does not include MD search procedures, to obtain the local minimum of the initial structure and to explore other regions in phase space that might lead to lower energy structures. Hence, we cannot exclude the possibility that the optimized structures obtained here are not real global minima. In the QM/MM calculations, however, the final energy refers to the perturbed QM energy, in the present case, the MP2 energy of $Fe(H_2O)_6{}^{3+/2+}$ and $UO_2(H_2O)_5{}^{2+/+}$. The different orientation of TIP3P waters has a rather limited effect in our case where the spherical solute with a saturated first shell is coordinated only with waters. Our problem is more associated with fixing charges on MM waters and this problem will be discussed later.

The structure of $UO_2(H_2O)_5{}^{2+}$ and $UO_2(H_2O)_5{}^{+}$ and their second hydration spheres are given in Figure 2. The main structural difference between U(VI) and U(V) is that there is no water molecule that is hydrogen-bonded to the axial oxygen in the former, whereas three TIP3P water molecules are bonded to two "-yl" oxygens in the latter due to the large negative charge on the "-yl" oxygens. This feature is identical to what Vallet et al.[35] have found through fully quantum mechanical calculations, and Hagberg et al.[45] through combined quantum mechanical and molecular dynamics simulations.

The reaction energy for reaction 3 obtained with the PCM model at the UMP2 level (without spin−orbit and thermal corrections) is 116.5 kJ/mol, as calculated from the data in Tables 2 and 5 (the corresponding result at the CASPT2 level is 67.5 kJ/mol).
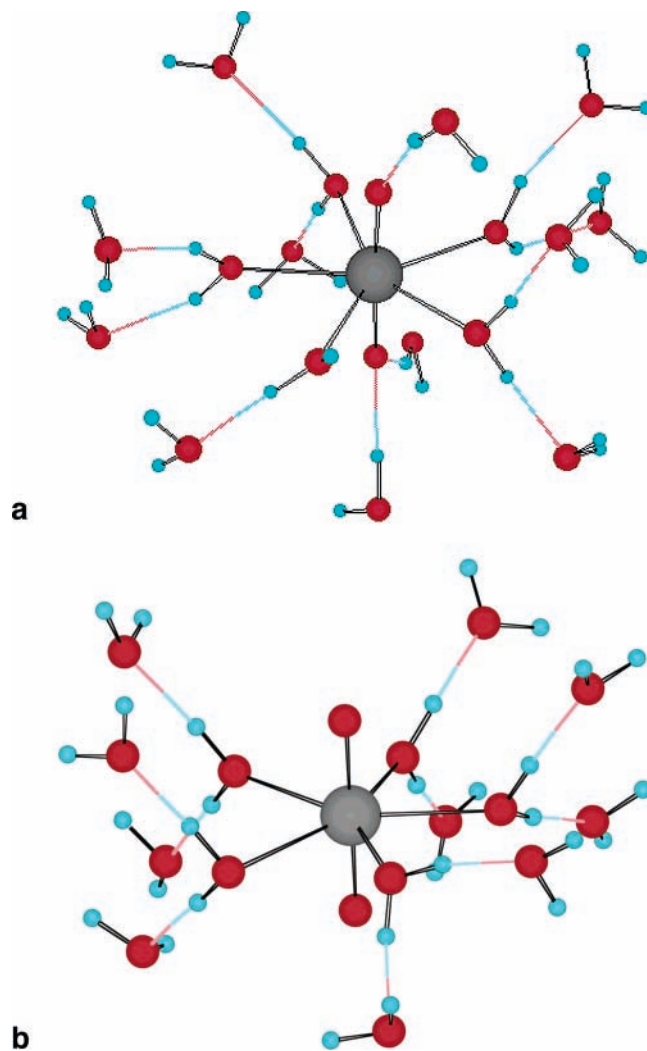

Figure 2. Structures of QM/MM optimized UO_2^+ (a) and UO_2^{2+} (b). Only first and second hydration shells and apical waters are shown in the figure.
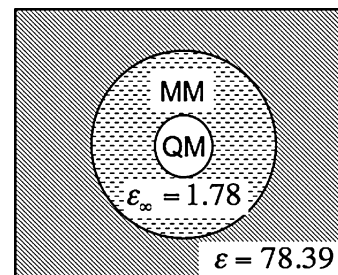

Figure 3. Concept of QM/MM calculation combined with classical Born formula. Solvation outside the QM/MM sphere was corrected with the static dielectric constant of water, $\epsilon = 78.39$. The MM region in the QM/MM part was corrected with the dynamic dielectric constant of water, $\epsilon_\infty = 1.78$.

The reaction energy of reaction 6 calculated by QM/MM method is +331.8 kJ/mol, before addition of corrections due to long-range polarization and the electronic response of the medium. The calculation with QM/MM using 1304 TIP3P waters as bulk waters corresponds to an about 30 Å "box size"; the contribution from the rest of the solvation sphere was estimated using the classical Born formula (eq 4) with the dielectric constant of water at room temperature, $\epsilon = 78.39$ (Figure 3). The long-range effect was modest, 71 kJ/mol, resulting in a reaction energy of +260.4 kJ/mol, which still is

TABLE 7: Calculated Reaction Energy (kJ/mol) of Aqueous $[UO_2(H_2O)_5]^{2+} + [Fe(H_2O)_6]^{2+} \rightarrow [UO_2(H_2O)_5]^+ + [Fe(H_2O)_6]^{3+}$ Using the QM/MM Method[a]

method	reaction energy
QM/MM only	+331.8
QM/MM + rest of solvation sphere ($\epsilon_0 = 78.39$)	+260.4
QM/MM + rest of solvation sphere ($\epsilon_0 = 78.39$) + dynamic solvation in MM region ($\epsilon_\infty = 1.78$)	+107.8
QM/PCM	+123.3

[a] Corrections using the Born formula are added. Spin−orbit effect, multireference correction, zero-point energy corrections, thermal corrections, and entropy effect are not added here. QM/PCM energies using the same ECP and basis sets are also shown in the table.

far from the PCM result. The TIP3P water molecules are not allowed to polarize, but as described in the method section, this effect can be mimicked by the Born formula (eq 5). This effect is quite large, 153 kJ/mol, and the final estimate of the solvent effect on the reaction energy (excluding spin−orbit effects and the thermodynamic corrections) is 107.8 kJ/mol, in reasonable agreement with the corresponding PCM result, 123.3 kJ/mol (Table 7). Charge fitting according to the Merz−Singh−Kollman scheme[46] was also tested against the Mulliken charge for comparison. However, change of the MM charge on the solute did change the reaction energy by less than 10 kJ/mol so the effect of solute MM charge in QM/MM calculation is minor as far as total reaction energy is concerned.

4. Conclusions

We have calculated the reduction potentials of Fe^{3+}/Fe^{2+} and AnO_2^{2+}/AnO_2^+ (An = U, Np, Pu, Am) at the CASPT2 and CCSD(T) levels using a cluster model where only the first hydration shell is explicitly included and the rest is described by polarizable conductor model (PCM).

The reduction potential calculated at the CASPT2 level by including spin−orbit effects, thermal corrections, and PCM solvation energy was in reasonable agreement with experimental values; the differences were all within 35 kJ/mol, which is slightly better than recently obtained DFT/PCM results.[15] The enthalpy change of the reactions were within 25 kJ/mol from the experimental values at the CASPT2 level, and within 5 kJ/mol at the CCSD(T) level. The present calculations indicate that it is not necessary to include second and higher coordination spheres in the solutes, and the PCM model was found to work well for reaction energy calculations of the present type. Previously, we found that PCM tends to overestimate the solvation energy for the outer-sphere electron-transfer reaction of $NpO_2^+ - NpO_2^{2+}$ in which the first hydration sphere is not saturated.[47] However, this seems to be associated with the difficulty in using a nonequilibrium PCM on the charge-separated $NpO_2^+ - NpO_2^{2+}$ system. Spin−orbit effects were found to be important for the actinides and may change ground-state configurations. The spin−orbit lowering of the ground-state energy does not increase with increasing number of unpaired f electrons but shows a more complicated trend as was found in the Pu(VI)/Pu(V) and Am(VI)/Am(V) cases.

Solvent effects on the reaction energies were very large, and to investigate the reliability of the PCM model in the present context we calculated the solvent effect on the reaction

$$UO_2^{2+}(aq) + Fe^{2+}(aq) \rightarrow UO_2^+(aq) + Fe^{3+}(aq)$$
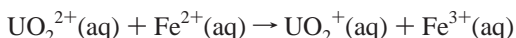
with both the PCM model and by QM/MM. The solvation energy calculation of highly charged cations such as $UO_2(H_2O)_5^{2+}$ or $Fe(H_2O)_6^{3+}$ using QM/MM method requires a very

large number of solvent molecules to describe long-range Coulomb interactions and, in addition, functions describing the electronic response of the solvent molecules. The effect of both long-range Coulomb interactions and electronic response can be estimated using the classical Born formula. With these corrections, the total reaction energy differed by 20 kJ/mol, which is acceptable. The results of the QM/MM calculations make it probable that the PCM model is capable of describing charge transfer reactions also for highly charged systems.

Supporting Information Available: Tables of the entropy in the gas phase and enthalpy and Gibbs energy correction of the complexes. This material is available free of charge via the Internet at http://pubs.acs.org.

References and Notes

(1) Katz, J. J.; Seaborg, G. T.; Morss, L. R. *The Chemistry of the Actinide Elements*, 2nd ed.; Chapman and Hall: New York, 1986.

(2) Wahlgren, U.; Tsushima, S.; Grenthe, I. *J. Phys. Chem. A* **2006**, *110*, 9025.

(3) Tomiyasu, H.; Fukutomi, H. *Bull. Chem. Soc. Jpn.* **1975**, *48*, 13.

(4) Newton, T. W. *The Kinetics of the Oxidation−Reduction Reactions of Uranium, Neptunium, Plutonium, and Americium in Aqueous Solutions*; Technical Information Center, Office of Public Affairs, U.S. Energy and Development Administration: Washington, DC, 1975.

(5) Privalov, T.; Schimmelpfennig, B.; Wahlgren, U.; Grenthe, I. *J. Phys. Chem. A* **2003**, *107*, 587.

(6) (a) Grenthe, I.; Fuger, J.; Konigs, R. J. M.; Lemire, R. J.; Muller, A. B.; Nguyen-Trung, C.; Wanner, H. *Chemical Thermodynamics of Uranium*; Elsevier Science Publishing Co., Inc.: New York, 1992; Vol. 1. (b) Silva, R. J.; Bidoglio, G.; Rand, M. H.; Robouch, P. B.; Wanner, H.; Puigdomenech, I. *Chemical Thermodynamics of Americium*; Elsevier Science Publishing Co., Inc.: New York, 1995; Vol. 2. (c) Lemire, R.; Fuger, J.; Nitsche, H.; Potter, P.; Rand, M. H.; Rydberg, J.; Spahiu, K.; Sullivan, J. C.; Ullman, W. J.; Vitorge, P.; Wanner, H. *Chemical Thermodynamics of Neptunium and Plutonium*; Elsevier Science Publishing Co., Inc.: New York, 2001; Vol. 4. (d) Guillaumont, R.; Fanghänel, T.; Fuger, J.; Grenthe, I.; Neck, V.; Palmer, D. A.; Rand, M. H. *Update on the Chemical Thermodynamics of Uranium, Neptunium, Plutonium, Americium and Technetium*; Elsevier Science Publishing Co., Inc.: New York, 2003; Vol. 5.

(7) Schumb, W. C.; Sherrill, M. S.; Sweetser, S. B. *J. Am. Chem. Soc.* **1937**, *59*, 2360.

(8) Whittemore, D. O.; Langmuir, D. *J. Chem. Eng. Data* **1972**, *17*, 288.

(9) Tsushima, S.; Yang, T. X.; Suzuki, A. *Chem. Phys. Lett.* **2001**, *334*, 365.

(10) Yang, T. X.; Tsushima, S.; Suzuki, A. *J. Phys. Chem. A* **2001**, *105*, 10439.

(11) Tsushima, S.; Reich, T. *Chem. Phys. Lett.* **2001**, *347*, 127.

(12) Wahlgren, U.; Moll, H.; Grenthe, I.; Schimmelpfennig, B.; Maron, L.; Vallet, V.; Gropen, O. *J. Phys. Chem. A* **1999**, *103*, 8257.

(13) Vallet, V.; Wahlgren, U.; Schimmelpfennig, B.; Szabó, Z.; Grenthe, I. *J. Am. Chem. Soc.* **2001**, *123*, 11999.

(14) Vallet, V.; Wahlgren, U.; Schimmelpfennig, B.; Moll, H.; Szabó, Z.; Grenthe, I. *Inorg. Chem.* **2001**, *40*, 3516.

(15) Shamov, G. A.; Schreckenbach, G. *J. Phys. Chem. A* **2005**, *109*, 10961.

(16) Hay, P. J.; Martin, R. L.; Schreckenbach, G. *J. Phys. Chem. A* **2000**, *104*, 6259.

(17) Li, J.; Fisher, C. L.; Chen, J. L.; Bashhold, D.; Noodleman, L. *Inorg. Chem.* **1996**, *35*, 4694.

(18) Uudsemaa, M.; Tamm, T. *J. Phys. Chem. A* **2003**, *107*, 9997.

(19) Frisch, M. J.; et al. *Gaussian 03*, revision C.02; Gaussian, Inc.: Pittsburgh, PA, 2003.

Tsushima et al.

(20) Karlström, G.; Lindh, R.; Malmqvist, P-Å.; Roos, B. O.; Ryde, U.; Veryazov, V.; Widmark, P.-O.; Cossi, M.; Schimmelpfennig, B.; Neogrady, P.; Seijo, L. *Comput. Mater. Sci.* **2003**, *28*, 222.

(21) Küchle, W.; Dolg, M.; Stoll, H.; Preuss, H. *J. Chem. Phys.* **1994**, *100*, 7535.

(22) Dolg, M.; Wedig, U.; Stoll, H.; Preuss, H. *J. Chem. Phys.* **1987**, *86*, 866.

(23) Krishnan, R.; Binkley, J. S.; Seeger, R.; Pople, J. A. *J. Chem. Phys.* **1980**, *72*, 650.

(24) (a) Hess, B. A.; Marian, C. M.; Wahlgren, U.; Gropen, O. *Chem. Phys. Lett.* **1996**, *251*, 365. (b) Marian, C. M.; Wahlgren, U. *Chem. Phys. Lett.* **1996**, *251*, 357.

(25) Schimmelpfennig, B. AMFI, an Atomic Mean-Field Integral program, Stockholm University, 1996.

(26) Küchle, W. Diplomarbeit, 1993.

(27) Schimmelpfennig, B.; Maron, L.; Wahlgren, U.; Teichteil, C.; Fagerli, H.; Gropen, O. *Chem. Phys. Lett.* **1998**, *286*, 267.

(28) (a) Barone, V.; Cossi, M. *J. Phys. Chem. A* **1998**, *102*, 1995. (b) Cossi, M.; Rega, N.; Scalmani, G.; Barone, V. *J. Comput. Chem.* **2003**, *24*, 669.

(29) (a) Maseras, T.; Morokuma, K. *J. Comp.Chem.* **1995**, *16*, 1170. (b) Humbel, S.; Sieber, S.; Morokuma, K.; *J. Chem. Phys.* **1996**, *105*, 1959. (c) Matsubara, T.; Sieber, S.; Morokuma, K. *Int. J. Quantum Chem.* **1996**, *60*, 1101.

(30) These basis sets are unpublished, but their use has been described in Ortiz, J. V.; Hay, P. J.; Martin, R. L. *J. Am. Chem. Soc.* **1992**, *114*, 2736.

(31) (a) Jorgensen, W. L.; Chandrasekhar, J.; Madura, J. D.; Impey, R. M.; Klein, M. L. *J. Chem. Phys.* **1983**, *79*, 926. (b) Kowall, T.; Foglia, F.; Helm, L.; Merbach, A. E. *J. Am. Chem. Soc.* **1995**, *117*, 3790.

(32) Turner, J. F. C.; Soper, A. K. *Polyhedron* **2004**, *23*, 2975.

(33) Guilbaud, P.; Wipff, G. *J. Phys. Chem.* **1993**, *97*, 5685.

(34) Born, M. Z. *Phys.* **1920**, *I*, 45.

(35) Vallet, V.; Privalov, T.; Wahlgren, U.; Grenthe, I. *J. Am. Chem. Soc.* **2004**, *126*, 7766.

(36) Benfatto, M.; Solera, J.; Ruiz, J. G.; Chaboy, J. *Chem. Phys.* **2002**, *282*, 441.

(37) Allen, P. G.; Bucher, J. J.; Shuh, D. K.; Edelstein, N. M.; Reich, T. *Inorg. Chem.* **1997**, *36*, 4676.

(38) Thompson, H. A.; Brown, G. E., Jr.; Parks, G. A. *Am. Mineral.* **1997**, *82*, 483.

(39) Reich, T.; Bernhard, G.; Geipel, G.; Funke, H.; Hennig, C.; Rossberg, A.; Matz, W.; Schell, N.; Nitsche, H. *Radiochim. Acta* **2000**, *88*, 633.

(40) Ankudinov, A. L.; Conradson, S. D.; de Leon, J. M.; Rehr, J. J. *Phys. Rev. B* **1998**, *57*, 7518.

(41) Conradson, S. D. *Appl. Spectrosc.* **1998**, *52*, 252A.

(42) Vallet, V.; Macak, P.; Wahlgren, U.; Grenthe, I. *Theor. Chem. Acc.* **2006**, *115*, 145.

(43) Matsika, S.; Zhang, Z.; Brozell, S.R.; Blaudeau. J.-P.; Wang, Q.; Pitzer, R. M. *J. Phys. Chem. A* **2001**, *105*, 3825.

(44) Martin, R. L.; Hay, P. J.; Pratt, L. R. *J. Phys.Chem. A* **1998**, *102*, 3565.

(45) Hagberg, D.; Karlström, G.; Roos, B. O.; Gagliardi, L. *J. Am. Chem. Soc.* **2005**, *127*, 14250.

(46) (a)Besler, B. H.; Merz, K. M., Jr.; Kollman, P. A. *J. Comput. Chem.* **1990**, 11, 431. (b) Singh, U. C.; Kollman, P. A. *J. Comput. Chem.* **1984**, *5*, 129.

(47) Macak, P.; Fromager, E.; Privalov, T.; Schimmelpfennig, B.; Grenthe, I.; Wahlgren, U. *J. Phys. Chem. A* **2005**, *109*, 4950.